UV Resonance Raman Spectroscopic Studies on the Genesis of Highly Dispersed Surface Molybdate Species on γ-Alumina

Guang Xiong, Zhaochi Feng, Jian Li, Qihua Yang, Pinliang Ying, Qin Xin, and Can Li*

State Key Laboratory of Catalysis, Dalian Institute of Chemical Physics, Chinese Academy of Sciences, P.O. Box 110, Dalian 116023, China

Received: October 11, 1999; In Final Form: January 18, 2000

The surface molybdate species and their coordination structures on γ- alumina are characterized by UV resonance Raman spectroscopy and UV−vis diffuse reflectance spectroscopy. The surface tetrahedral and octahedral molybdate species can be definitely identified on the basis of the resonance Raman effect. The evolution of surface species has been studied during the catalyst preparation under various conditions including the pH value of the impregnating solution and the pretreatment temperature. It is shown that the coordination structures of the supported molybdate in the wet state are dependent on the structures of molybdate in the impregnation solution as well as the surface property of γ-alumina. When the impregnating solution is at pH = 10.0, only tetrahedral molybdate species are formed on γ-alumina, while both tetrahedral and octahedral species are formed on γ-alumina at pH = 3.0, although the molybdate is in only the octahedral form in the impregnation solution at pH = 3.0. For the samples prepared by the impregnating solution of $(NH_4)_6Mo_7O_{24}$, some surface tetrahedral molybdate species polymerize to the octahedral species during calcination even when the loading of molybdate is extremely low. However, the surface molybdate species hardly aggregate into the octahedral species when the sample prepared by the impregnating solution of Na_2MoO_4. It turns out that the "surface pH value" (i.e., the pH value of surface region) is a key factor governing the coordination structure of the surface molybdate species.

Introduction

Highly dispersed metal oxides on the supports, such as Al_2O_3 or SiO_2 with high surface area, are a class of important catalysts widely used in chemical industry processes. [1,2] These catalysts are usually prepared by impregnating the supports with the solution containing the salts of the metal. The study on the genesis of the surface metal oxide species will lead to the deeper insights into the nature of the surface active sites and active phases which are responsible for the catalytic performance.

Among the metal oxide catalysts, supported molybdenum oxide has drawn much attention because it has been widely used as the catalysts and catalyst precursors for many reactions. [3−11] It is also a kind of model catalysts for studying the interaction between the metal oxide species and the support surface. The structures of the supported molybdenum oxide have been investigated by many techniques. [12−16] However, the techniques such as Auger spectroscopy, X-ray photoelectron spectroscopy (XPS), and electron-spin resonance (ESR) only give mainly the information on the atoms in oxide but the oxide structure. X-ray diffraction (XRD) gives mainly the information on the bulk oxide but the highly dispersed species. Raman spectroscopy is one of the proper techniques used for the characterization of the supported oxides catalysts since the Raman signals can give the direct information on the surface coordination structures of the supported metal oxide species. [17−19]

In the past, a lot of Raman work [20−34] has been focused on the MoO_3/γ-Al_2O_3 catalyst. Two kinds of coordination structures of surface molybdate species, the tetrahedral and the octahedral species, have been found to be present on γ-alumina.[30−32] The tetrahedral molybdenum oxide is associated with the isolated species, while the octahedral molybdate is the polymerized species. The coordination structures of the surface molybdate, which contributes the activity and selectivity of the catalytic reactions, could be controlled by the preparation procedure and method.

The evolution of the surface molybdate during preparation is still controversial although it has been studied extensively. Jeziorowski and Knözinger [24] suggested that only the MoO_4^{2-} species was formed on the support in the wet state despite the pH value of the impregnating solution, and the tetrahedral species was polymerized into the octahedral species after a calcination. Wang and Hall [26] indicated that the adsorbed molybdate species in the wet state was dependent on the pH value of the impregnating solution. The tetrahedral molybdate species adsorbed on γ-Al_2O_3 at high pH value, while the octahedral species was formed at low pH value. Wachs [18] demonstrated that the molecular structures of the hydrated surface metal oxide species are related to the net pH value at which the surface possesses zero surface charge (the point of zero charge).

The Raman study of the supported molybdate has been limited to the low loading of molybdate because of the low sensitivity and the strong fluorescence interference of conventional Raman spectroscopy. Recent studies [35−42] showed that UV resonance Raman spectroscopy is a powerful tool for the study of the catalysts and other solids. Our previous paper [42] has demonstrated that UV resonance Raman spectroscopy is a very sensitive technique for the characterization of the coordination structures of supported molybdate even with extremely low loading. This makes it possible to get the knowledge of the

* Telephone: 86-411-4671991 ext. 728. Fax: 86-411-4694447 or 4691570. E-mail: canli@ms.dicp.ac.cn.

10.1021/jp993609z CCC: $19.00
Published on Web 03/28/2000

TABLE 1: Preparation of the MoO_3/γ-Al_2O_3 Samples Using Equilibrium Adsorption Method

MoO_3/γ-Al_2O_3[a] sample	pH value	MoO_3 loading (wt %)
MoO_3/γ-Al_2O_3 (10)	10.0	0.3
MoO_3/γ-Al_2O_3 (6)	6.0	4.7
MoO_3/γ-Al_2O_3 (3)	3.0	10.8

[a] The concentration of molybdate in the solution is 4.0×10^{-3} M.

interaction between the surface molybdate species and the support particularly when the concentration of the surface molybdate species is very low.

In this work the evolution of the MoO_3/γ-Al_2O_3 during the preparation was investigated by the UV resonance Raman spectroscopy together with the UV−vis diffuse reflectance spectroscopy. The fluorescence-free spectra with high sensitivity are obtained using UV laser line as the excitation source. The coordination structures of two molybdate species, tetrahedral and octahedral, are identified on the basis of the resonance Raman effect by using the laser lines at 244 and 325 nm. It is found that the coordination structures of the surface species are apparently controlled by the pH value of the impregnation solution, the net pH value at PZC of the support, and the calcination temperature, but essentially controlled by the net pH value at the surface region of the support.

Experimental Section

Catalyst Preparation. The supported molybdate was prepared by the equilibrium adsorption method. γ-Al_2O_3 (S_{BET} = 242 m^2/g, Phôe-Poulence) was used as the support. Impregnating solutions of molybdate at pH = 3.0, 6.0 and 10.0 were adjusted by adding HNO_3 or NH_4OH. γ-Al_2O_3 was impregnated in an aqueous solution of ammonium heptamolybdate (AHM). The aqueous solution with AHM was stirred for enough time to reach the equilibrium adsorption. The impregnated support was filtered, then dried at room temperature and 393 K, and finally calcined at 773 K. The weight loadings of the samples are given in Table 1. The samples prepared at pH = 10.0, 6.0, and 3.0 are denoted as MoO_3/γ-Al_2O_3 (10), MoO_3/γ-Al_2O_3 (6), and MoO_3/γ-Al_2O_3 (3), respectively, although the surface molybdate-containing species in the wet and dried samples are not exactly in the form of MoO_3. UV resonance Raman spectra of the samples were recorded under ambient conditions at three stages: wet (dried at room temperature), dried (dried at 393 K), and calcined (calcined at 773 K) states.

UV Resonance Raman Spectroscopy. UV resonance Raman spectra were obtained on a homemade UV resonance Raman spectrograph. The spectrograph has four main parts: an UV cw laser, a spex 1877 D triplemate spectrograph, a CCD detector, and an optical collection system. A 244.0-nm line from an Innova 300 FRED laser and a 325.0-nm line of a He−Cd laser were used as the excitation sources. The 244.0-nm line is generated by frequency doubling of the 488.0-nm line via a cw intracavity frequency doubled Ar-ion laser. The power of the laser lines, measured at the samples, were below 4.0 mW for 244.0 nm and 1.0 mW for 325.0 nm, respectively. Samples were mounted into a spinning holder to avoid thermal damage during the spectrum scanning which usually takes about 5 min. The spectral resolution was estimated to be 2.0 cm^{-1}.

Ultraviolet−Vis Diffuse Reflectance Spectroscopy. UV−vis diffuse reflectance spectra of the samples were recorded on a Shimadzu UV-365 UV−Vis−NIR Spectrophotometer. The spectra were collected against a pure alumina as a reference.

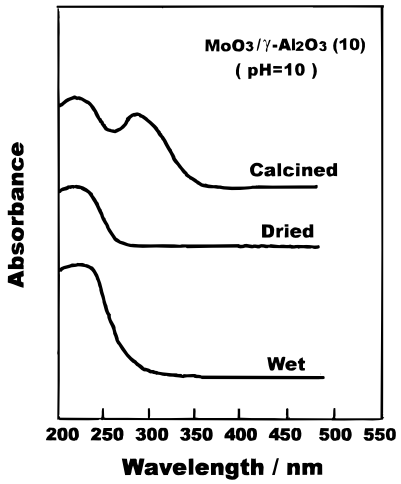

Figure 1. UV−vis diffuse reflectance spectra of MoO_3/γ-Al_2O_3 (10) sample prepared at pH = 10.0 using equilibrium adsorption method with the solution of $(NH_4)_6Mo_7O_{24}$.

Results

UV−Vis Diffuse Reflectance Spectra. *(a) MoO_3/γ-Al_2O_3 (10) Sample.* The UV−vis diffuse reflectance spectra of the wet, dried and calcined MoO_3/γ-Al_2O_3 (10) samples are shown in Figure 1. The wet and dried MoO_3/γ-Al_2O_3 (10) samples give only a UV absorption at 240 nm, while the calcined MoO_3/γ-Al_2O_3 (10) sample exhibits two UV−Vis absorptions at 240 and 290 nm.

It has been assigned that the band at 230−260 nm is the characteristic absorption of Mo═O bond of tetrahedral molybdate and the band at about 320 nm is due to the Mo−O−Mo bridge bond of octahedral species. [43−56] The band at 280 nm has been ascribed to the monomer, dimmer or polymerized molybdate species, but the exact assignment is still not clear yet. [23,53,54] As shown in Figure 1, the absorption at 240 nm is detected for MoO_3/γ-Al_2O_3 (10) sample in the wet and dried states. This may imply that the tetrahedral molybdate species alone exists on γ-Al_2O_3 in the wet and the dried states. The absorption at 290 nm in Figure 1 may be due to the overlap of the bands at 280 and 320 nm. The appearance of the absorptions at 240 and 290 nm after the calcination possibly indicates that the tetrahedral molybdate species together with the octahedral species are formed on the support. This suggests that some tetraheral molybdate species may polymerize into the octahedral species during the calcination.

(b) MoO_3/γ-Al_2O_3 (6) Sample. The UV−vis diffuse reflectance spectra of MoO_3/γ-Al_2O_3 (6) samples in the wet, dried and calcined states are presented in Figure 2. The MoO_3/γ-Al_2O_3 (6) sample in the wet state exhibits a broad band at 220−350 nm. This band can be considered as the overlap of the absorption bands at 240, 280 and 320 nm. This broad band probably indicates that both the tetrahedral and the octahedral molybdate are formed in the wet state on the support. After the drying and calcination, the band becomes broadened and its tail extends to 400 and 450 nm, respectively. It has been suggested that the broadening and the red shift of the lowest energy transition absorption of molybdate correspond to the molybdate cluster with larger size. [55] Therefore, this assumes the formation of aggregated molybdate species after the calcination.

(c) MoO_3/γ-Al_2O_3 (3) Sample. Figure 3 gives the UV−vis diffuse reflectance spectra of the MoO_3/γ-Al_2O_3 (3) sample in the wet, dried and calcined states. UV resonance Raman spectrum of the MoO_3/γ-Al_2O_3 (3) sample in the wet state exhibits a broad band between 220 and 350 nm. This is very

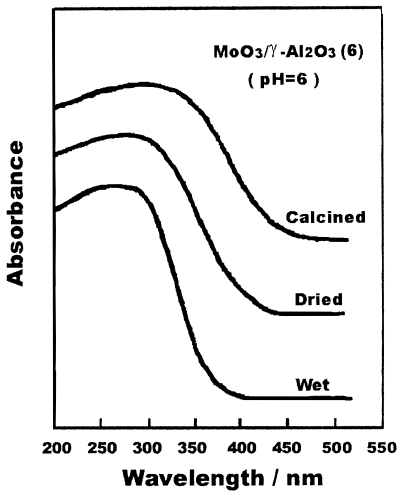

Figure 2. UV−vis diffuse reflectance spectra of MoO_3/γ-Al_2O_3 (6) sample prepared at pH = 6.0 using equilibrium adsorption method with the solution of $(NH_4)_6Mo_7O_{24}$.

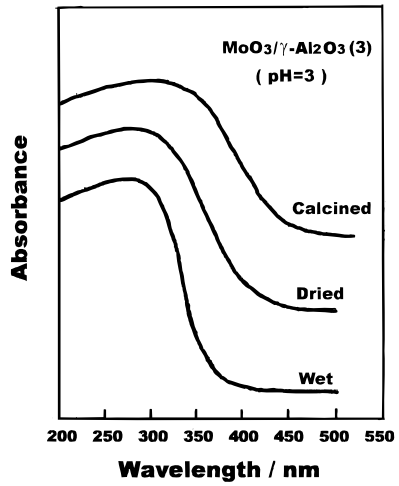

Figure 3. UV−vis diffuse reflectance spectra of MoO_3/γ-Al_2O_3 (3) sample prepared at pH = 3.0 using equilibrium adsorption method with the solution of $(NH_4)_6Mo_7O_{24}$.

similar to that of MoO_3/γ-Al_2O_3(6); namely, both tetrahedral and octahedral molybdate species are present on the surface. After drying and calcination, the absorption band becomes broad and its tail shifts to 400 and 450 nm, respectively. As we have discussed above, this probably suggests that both the tetrahedral and octahedral molybdate species are formed on the support in the wet state, and the surface molybdate species polymerizes further after the drying and calcination.

UV Resonance Raman Spectra of MoO_3/γ-Al_2O_3 Samples. *(a) Molybdate Species in the Impregnating Solution Excited by 244 nm.* Figure 4 shows UV resonance Raman spectra of molybdate species in the impregnating solution (aqueous solution of ammonium heptamolybdate) at different pH values excited by the laser line at 244 nm. The Raman bands at 837, 897, 1784, and 2674 cm^{-1} are observed for the molybdate species in the solution at pH = 10.0. The assignments of the Raman bands of the molybdate species are given in Table 2. The bands at 837 and 897 cm^{-1} are attributed to the stretching modes of Mo═O bond of the tetrahedral molybdate species. The bands at 1784 and 2674 cm^{-1}, being not observed in normal Raman spectra, are detected in UV resonance Raman spectra. Considering the fact that the laser line at 244 nm excites the charge-transfer absorption of Mo═O bond, the bands at 1784 and 2674 cm^{-1} can be assigned to the double and triple

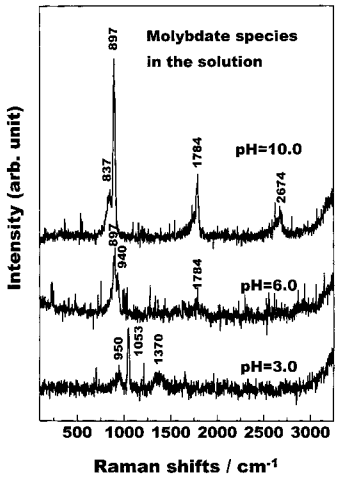

Figure 4. UV resonance Raman spectra of molybdate species in the impregnating solution at different pH values excited by the laser line at 244 nm.

TABLE 2: The Assignment of the Raman Bands of Molybdate (ref 32)

symmetry	compound	((Mo−O−Mo)	((Mo−O)	((Mo═O)	((Mo═O)
T_d	MoO_4^{2-}		317	837	897
T_d and O_h	$K_2Mo_2O_7$	196	335		927
O_h	$Mo_7O_{24}^{6-}$	219	362	903	943
O_h	$Mo_8O_{26}^{4-}$	230	370	925	965

frequencies of symmetric stretching of the Mo═O mode of tetrahedral molybdate species owing to the resonance Raman effect. [42]

The Raman bands at 897, 940, and 1784 cm^{-1} appear in the UV resonance Raman spectrum of molybdate species in the solution at pH = 6.0. The bands at 897 and 1784 cm^{-1} are attributed to tetrahedral molybdate species. The band at 940 cm^{-1} is assigned to the symmetric stretching mode of Mo═O bond of the octahedral species. This suggests that both tetrahedral and octahedral molybdate species coexist in the solution at pH = 6.0.

There are three Raman bands at 950, 1053, and 1370 cm^{-1} detected for the molybdate species in the solution at pH = 3.0. The band at 950 cm^{-1} is assigned to the octahedral molybdate species. The bands at 1053 and 1370 cm^{-1} are due to the NO_3^- species because HNO_3 was added for adjusting the pH value of the solution.

(b) MoO_3/γ-Al_2O_3 (10) Excited by 244 nm. UV resonance Raman spectra of the MoO_3/γ-Al_2O_3 (10) sample excited by the laser line at 244 nm are presented in Figure 5. There are four Raman bands at 320, 897, 1786, and 2679 cm^{-1} for the wet sample. The bands at 320 and 897 cm^{-1} are respectively assigned to the bending and symmetric Mo═O stretching modes of the tetrahedral molybdate species. The bands at 1786 and 2679 cm^{-1} are assigned to the double and triple frequencies of symmetric stretching of Mo═O mode of tetrahedral molybdate species.

As shown in Figure 5, the band at 320 cm^{-1} shifts to 325 cm^{-1} after drying at 393 K. At the same time the band at 897 cm^{-1} is splitted into the doublet peaks at 900 and 916 cm^{-1}. Similarly, the bands at 1786 and 2679 cm^{-1} are also splitted into two doublet bands at 1782, 1827 and 2678, 2745 cm^{-1}, respectively. This suggests that the tetrahedral molybdate species on the surface is distorted after the drying at 393 K.

After the calcination at 773 K, the band at 320 cm^{-1} in the wet state shows a further shift to 335 cm^{-1}. (see Figure 5) The bending band at 335 cm^{-1} is broad and locates between the

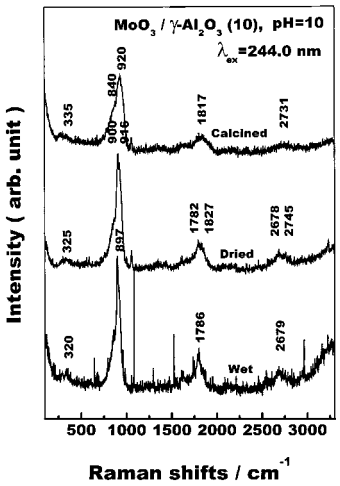

Figure 5. UV resonance Raman spectra of MoO_3/γ-Al_2O_3 (10) sample prepared at pH = 10.0 excited by the laser line at 244.0 nm.

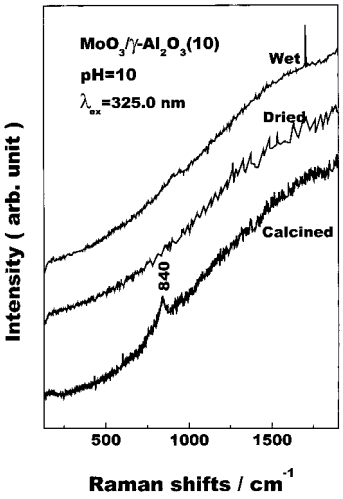

Figure 6. UV resonance Raman spectra of MoO_3/γ-Al_2O_3 (10) sample prepared at pH = 10.0 excited by the laser line at 325.0 nm.

band at 320 cm^{-1} of the tetrahedral molybdate species and the band at 360 cm^{-1} of the octahedral species. This band can be assigned to the overlap of the bending bands of the tetrahedral and octahedral molybdate species. Simultaneously the bands associated with the Mo═O stretching mode shift from 897, 1786, and 2679 cm^{-1} to 920, 1817, and 2731 cm^{-1}, respectively. These bands become broaden in contrast with those in the wet and the dried states. A shoulder band at 840 cm^{-1} appears in the spectrum for the calcined state. This band is associated with the Mo−O−Mo asymmetric stretching mode of the octahedral molybdate species. These results demonstrate that some octahedral molybdate species begin to appear after the calcination.

(c) MoO_3/γ-Al_2O_3 (10) Excited by 325 nm. UV resonance Raman spectra of the MoO_3/γ-Al_2O_3 (10) sample using the laser line at 325 nm as the excitation source are shown in Figure 6. No Raman signals can be detected in the wet and dried state because of the interference of strong fluorescence background. A band at 840 cm^{-1} is detected after the calcination at 773 K. This band is attributed to the asymmetric stretching band of Mo−O−Mo bridge bond. The excitation line at 325 nm is accessible to the electronic absorption band of Mo−O−Mo bridge bond, hence the intensity of the 840 cm^{-1} band is increased by the resonance Raman effect. [42]

According to the results in Figures 1, 5, and 6, it is shown that only tetrahedral molybdate species is formed on γ-Al_2O_3 for MoO_3/γ-Al_2O_3 (10) sample in the wet state. The tetrahedral molybdate species becomes distorted after drying at 393 K, and the calcination at 773 K results in the aggregation of the tetrahedral molybdate species.

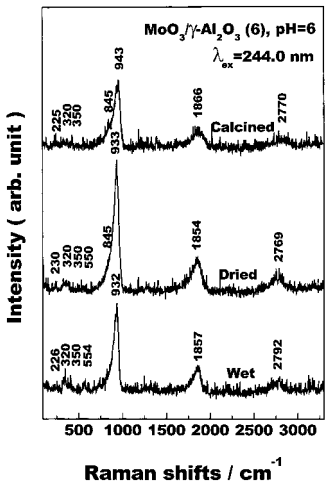

Figure 7. UV resonance Raman spectra of MoO_3/γ-Al_2O_3 (6) sample prepared at pH = 6.0 excited by the laser line at 244.0 nm.

(d) MoO_3/γ-Al_2O_3 (6) Excited by 244 nm. UV resonance Raman spectra of the MoO_3/γ-Al_2O_3 (6) sample excited by the laser line at 244 nm are shown in Figure 7. The Raman bands at 226, 320, 350, 554, 932, 1857, and 2792 cm^{-1} are detected for the MoO_3/γ-Al_2O_3 (6) sample in the wet state. The bands at 226, 350, and 554 cm^{-1} are assigned to the Mo−O−Mo deformation, Mo═O bending, and Mo−O−Mo symmetric stretching modes of the octahedral molybdate, respectively. A band at 320 cm^{-1} is attributed to the Mo═O bending mode of the tetrahedral molybdate. This indicates that both tetrahedral and octahedral species are formed on γ-alumina for MoO_3/γ-Al_2O_3 (6) catalyst in the wet state. The bands at 932, 1857, and 2792 cm^{-1} are attributed to the fundamental, double, and triple frequencies of Mo═O bond, respectively. The frequency position of 932 cm^{-1} is between 897 cm^{-1} of tetrahedral molybdate and 950 cm^{-1} of the octahedral species. The band at 932 cm^{-1} is possibly due to the overlap of the Mo═O symmetric stretching modes of surface tetrahedral and octahedral molybdate species.

After drying at 393 K, the bands at 1857 and 2792 cm^{-1} shift to 1854 and 2769 cm^{-1}, respectively. (see Figure 7) The intensity of the band at 320 cm^{-1} becomes weaker while that of the band at 350 cm^{-1} becomes stronger. This demonstrates that some tetrahedral molybdate are polymerized into the octahedral species after the drying.

After the calcination at 773 K, the fundamental, double and triple frequency modes of Mo═O bond shift from 932, 1857, and 2792 $cm^{-1}$of the wet sample to 943, 1866 and 2770 cm^{-1}, and become broaden as the pretreatment temperature increases. (see Figure 7) The intensity of a shoulder band at 845 cm^{-1} becomes stronger after the calcination. This manifests that the molybdate species with larger size is formed after the calcination.

(e) MoO_3/γ-Al_2O_3 (6) Excited by 325 nm. UV resonance Raman spectra of the MoO_3/γ-Al_2O_3 (6) sample using the laser line at 325.0 nm as the excitation source are given in Figure 8. The Raman bands in the finger region are obscured by the fluorescence background. Two bands at 905 and 945 cm^{-1} are detected for MoO_3/γ-Al_2O_3 (6) sample in the wet state. The band at 945 cm^{-1} is attributed to the symmetric stretching mode of Mo═O bond of the octahedral molybdate species, while the band at 905 cm^{-1} in Figure 8 should be assigned to the

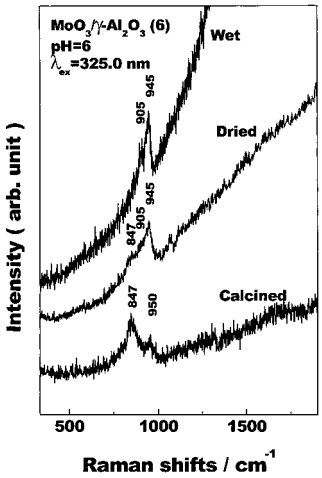

Figure 8. UV resonance Raman spectra of MoO_3/γ-Al_2O_3 (6) sample prepared at pH = 6.0 excited by the laser line at 325.0 nm.

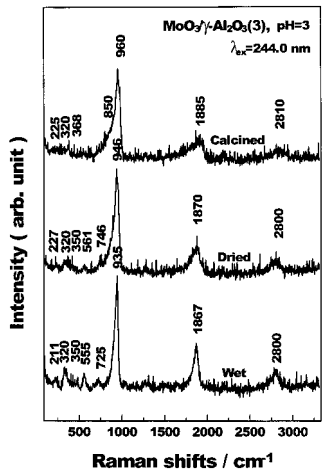

Figure 9. UV resonance Raman spectra of MoO_3/γ-Al_2O_3 (3) sample prepared at pH = 3.0 excited by the laser line at 244.0 nm.

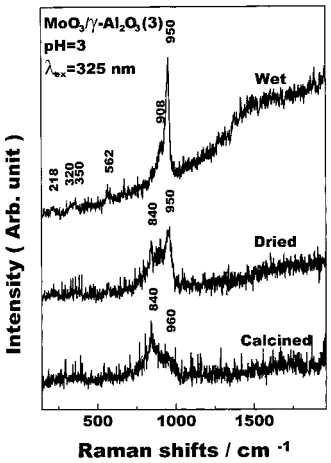

Figure 10. UV resonance Raman spectra of MoO_3/γ-Al_2O_3 (3) sample prepared at pH = 3.0 excited by the laser line at 325.0 nm.

symmetric stretching mode of Mo═O bond of the tetrahedral species. This result confirms that the Mo═O stretching band at 932 cm^{-1} in Figure 7 of the wet state is the overlap of the bands of the tetrahedral and octahedral molybdate.

After drying at 393 K, the Raman bands at 847 and 945 cm^{-1} and a shoulder band at 905 cm^{-1} appear in the spectrum of the MoO_3/γ-Al_2O_3 (6) sample. (see Figure 8) The intensity of the band at 905 cm^{-1} becomes weaker. This suggests that the amount of tetrahedral molybdate decreases. The new band at 847 cm^{-1} is attributed to the asymmetric stretching mode of the Mo−O−Mo bridge bond of the octahedral molybdate. The appearance of this band is due to the aggregation of the surface molybdate species.

As shown in Figure 7, the MoO_3/γ-Al_2O_3 (6) sample in the calcined state gives the Raman bands at 847 and 950 cm^{-1}. The intensity of the band at 847 cm^{-1} becomes stronger than that of the band at 950 cm^{-1}. The band 847 cm^{-1} is the resonance Raman band since the laser line at 325 nm excites the UV−vis absorption of the Mo−O−Mo bond. This can be explained in term of the transformation from tetrahedral to octahedral species during the calcination.

UV resonance Raman and UV−vis diffuse reflectance spectra of MoO_3/γ-Al_2O_3 (6) catalyst show that both tetrahedral and octahedral molybdate species are present on the support in the wet state. During the drying and calcining periods, the amount tetrahedral molybdate species decreases while that of the octahedral species increases owing to the polymerization of the surface species during the calcination.

(f) MoO_3/γ-Al_2O_3 (3) Excited by 244 nm. Raman spectra of the MoO_3/γ-Al_2O_3 (3) sample excited by the laser line at 244 nm are presented in Figure 9. The Raman bands at 211, 320, 350, 555, 725, 935, 1867, and 2800 cm^{-1} are present in the UV resonance Raman spectrum of the MoO_3/γ-Al_2O_3 (3) catalyst in the wet state. The band at 320 cm^{-1} is assigned to the bending mode of the tetrahedral molybdate. Raman bands at 211, 350, and 555 cm^{-1} are attributed to the octahedral species. This proposes that both the tetrahedral and the octahedral molybdate species are formed on γ-alumina in the wet state. The bands at 935, 1867, and 2800 cm^{-1} are attributed to the fundamental, double and triple frequencies of Mo═O stretching modes of the tetrahedral and octahedral molybdate species.

After a drying at 393 K the bands at 227, 320, 350, 561, 746, 946, 1870, and 2800 cm^{-1} are detected. (see Figure 9) The intensity of the band at 320 cm^{-1} becomes weaker while that of the band at 350 cm^{-1} is stronger after the drying. The Mo═O stretching mode shifts from 935 to 946 cm^{-1}. After being calcinied at 773 K, the MoO_3/γ-Al_2O_3 (3) sample exhibits Raman bands at 225, 320, 368, 850, 960, 1885 and 2810 cm^{-1}. (see Figure 9) The fundamental, double, and triple frequencies of the Mo═O stretching bands shift to 960, 1885, and 2810 cm^{-1}, respectively. The intensity of a shoulder band at 850 cm^{-1}, which is attributed to Mo−O−Mo asymmetric stretching mode, becomes stronger. These results imply that the amount and the size of the polymerized molybdate increase, while the amount of the tetrahedral species decreases during the drying and calcination pretreatment.

(g) MoO_3/γ-Al_2O_3 (3) Excited by 325 nm. UV resonance Raman spectra of the MoO_3/γ-Al_2O_3 (3) sample excited by the laser line at 325 nm are shown in Figure 10. The MoO_3/γ-Al_2O_3 (3) sample in the wet state gives the bands at 218, 320, 350, 562, 908, and 950 cm^{-1}. The bands at 218, 350 and 562 cm^{-1} are associated with the octahedral molybdate, and the band at 320 cm^{-1} is assigned to the tetrahedral molybdate species. The bands at 908 and 950 cm^{-1} are attributed to Mo═O symmetric stretching modes of the tetrahedral and the octahedral molybdate species, respectively. This suggests that both the tetrahedral and the octahedral molybdate species are formed on the support in the wet state. The fact that the intensity of the band at 908 cm^{-1} is much weaker than that of the band at 950 cm^{-1} indicates that the octahedral molybdate species is predominant on alumina in the wet state.

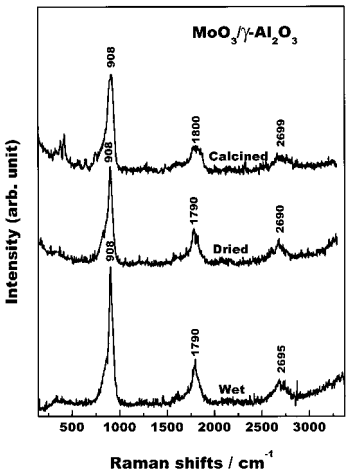

Figure 11. UV resonance Raman spectra of MoO_3/γ-Al_2O_3 sample prepared using the equilibrium adsorption method with the solution of Na_2MoO_4 excited by the laser line at 244.0 nm.

After being dried at 393 K, the MoO_3/γ-Al_2O_3 (3) sample exhibits Raman bands at 840, 908, and 950 cm^{-1}. (see Figure 10) The intensity of the band at 908 cm^{-1} is weaker and becomes broaden after the drying. After being calcinied at 773 K, the bands at 840 and 960 cm^{-1} are observed in Figure 10. A Mo−O−Mo asymmetric stretching band at 840 cm^{-1}, which is enhanced by resonance Raman effect, begins to appear when drying at 393 K and becomes stronger after the calcination at 773 K. The band at 950 cm^{-1} becomes broaden and shifts to 960 cm^{-1}. Similar to the results of the MoO_3/γ-Al_2O_3 (10) and the MoO_3/γ-Al_2O_3 (6) samples, transformation from isolated tetrahedral to polymerized octahedral molybdate occurs during the calcination.

From Figures 3, 9, and 10, both the tetrahedral and octahedral molybdate species are formed on the support in the wet state, while the octahedral molybdate species is predominant for the MoO_3/γ-Al_2O_3 (3) sample. In particular, the octahedral species prevails for the MoO_3/γ-Al_2O_3 sample resulting from the aggregation of the surface species during the calcination.

(h) MoO_3/γ-Al_2O_3 Sample Prepared by Using Na_2MoO_4. The UV resonance Raman spectra of MoO_3/γ-Al_2O_3 sample prepared by using Na_2MoO_4 are shown in Figure 11. The sample in the wet state gives the Raman bands at 320, 908, 1790, and 2695 cm^{-1}. These bands are attributed to the tetrahedral molybdate species. It is interesting that during drying and calcination, the Raman bands hardly shift, but just become slightly broader. This fact demonstrates that the tetrahedral molybdate do not aggregate together for the MoO_3/γ-Al_2O_3 prepared from the solution of Na_2MoO_4 even after the calcination.

Discussion

The distribution of the different molybdate species in its solution is strongly depend on the pH value:[17]

$$\underset{(pH=10)}{7MoO_4^{2-}} + 8H^+ \leftrightarrow \underset{(pH=3)}{Mo_7O_{24}^{6-}} + 4H_2O$$

The molybdate is in the form of the tetrahedral species at pH > 9.0, while only the octahedral species is present in the solution at pH < 5.5. Both the tetrahedral and octahedral molybdate species coexist in the solution at pH values between 5.5 and 9.0.[53] As confirmed in Figure 4, the molybdate species in the solution at pH = 3.0, 6.0, and 10.0 are in the forms of the $Mo_7O_{24}^{6-}$, both $Mo_7O_{24}^{6-}$ and MoO_4^{2-}, and MoO_4^{2-} species, respectively.

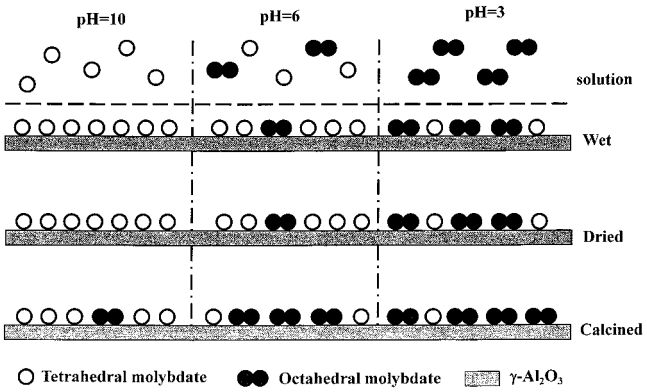

Figure 12. Schematic model of the evolution of the surface molybdate species during the preparation

At pH = 10, only the tetrahedral MoO_4^{2-} species are formed on the support after the adsorption. (see Figure 5) At pH value of 6.0, both tetrahedral and octahedral species are formed on γ-Al_2O_3 in the wet state. (see Figures 7 and 8) The molybdate species adsorbed on the support for the MoO_3/γ-Al_2O_3 (10) and the MoO_3/γ-Al_2O_3 (6) samples in the wet state are similar to that in the impregnating solution. However, the molybdate species on the support in the wet state are not always in consistent with that in the impregnating solution. Both the octahedral and the tetrahedral molybdate species are derived for MoO_3/γ-Al_2O_3 (3) sample (see Figures 9 and 10), although only the octahedral species exists in the impregnating solution at pH = 3. (see Figure 4) This indicates that some polymolybdate decompose when they interact with γ-Al_2O_3 in the strong acidic solution. A schematic model of the adsorption of the molybdate species on γ-Al_2O_3 is shown in Figure 12.

It has been suggested that the molybdate species may dissociate in the solution using the incipient wetness method because of the fairly large buffer capacity of the alumina support.[57,58] A study used Mo-95 NMR spectroscopy also demonstrated that the decomposition of $Mo_7O_{24}^{6-}$ to MoO_4^{2-} due to the increase in the pH value of the impregnating solution inside the pores of the alumina.[15] However, the volume of the solution used in the equilibrium adsorption method is rather large, and the final pH value of the solution in the equilibrium adsorption would not be altered too much.[53] Therefore, the polymolybdate cannot decompose into isolated species in the solution. We believe that the dissociation of the polymolybdate occurs only after it interacts with the support.

PZC (the point of zero charge) is defined as the concentration of the potential-determining ions at which the surface charge is zero. The surface species was suggested to be determined by the net pH value at which the surface possesses zero surface charge (PZC).[18] But the net pH value of the surface varies with the pH value of the impregnating solution because of the buffer effect of the surface. So a "surface pH value " is defined as the net pH value at the surface region. A "surface pH value" of the support in the impregnating solution is actually a function of the pH value at PZC of the sample and the pH value of the impregnating solution. The surface pH value of γ-Al_2O_3 at PZC is 8.0.[58] The "surface pH value" will be lower than 8.0 when the pH value of the impregnating solution is below 8.0 (e.g., pH value at 3.0 for sample MoO_3/γ-Al_2O_3 (3) and 6.0 for sample MoO_3/γ-Al_2O_3(6)). Both the tetrahedral and the octahedral molybdate species are formed on the support for the MoO_3/γ-Al_2O_3 (3) and MoO_3/γ-Al_2O_3 (6) samples in the wet state, since the "surface pH value" is lower than 8.0. The "surface pH value" of γ-Al_2O_3 should be higher than 8.0 when the pH value of the impregnating solution is around 10.0 after adjusting by NH_4·

OH. As a result, only the tetrahedral molybdate species is formed on the support. Therefore, the molybdate in the wet state is solely related to the "surface pH value" of the support.

To obtain further insight into the interaction between the surface species and the support, the surface property of γ-Al_2O_3 should be considered. There are five possible OH configurations on alumina. [62] The surface OH groups in the various configurations possess the different net charges, which result in their acidic or basic properties. IR studies suggested that the surface OH groups consumed sequentially upon deposition of the metal oxides. [63] The bands due to more basic hydroxyls disappear first. The bands due to neutral and acidic OH groups disappear at higher loadings of the metal oxide. An assumption may be used to explain how the polymolybdate decomposes on γ-Al_2O_3 even at pH = 3 for the impregnating solution. The adsorbed polymolybdate interacts with the basic hydroxide groups on γ-Al_2O_3. As a consequence, the polymolybdate decomposes to monomolybdate on the surface since this surface microenvironment is basic. When molybdate is adsorbed at pH = 6.0 and 3.0, the tetrahedral molybdate species on the support exhibit Raman bands at 905 and 908 cm^{-1}, respectively. (see Figures 8 and 10) The frequencies of these Raman bands are higher than that of MoO_4^{2-} species existed in the solution. The shift of the Mo−O symmetric stretching mode confirms that the tetrahedral molybdate are formed when the polymolybdate interacts with the basic hydroxyl groups of γ-Al_2O_3. The bands at 945 and 950 cm^{-1} of the polymolybdate are similar to those of $Mo_7O_{24}^{6-}$ in the solution. (see Figures 8 and 10) This suggests that the $Mo_7O_{24}^{6-}$ like species are physisorbed on the γ-Al_2O_3 in the impregnating solution. [59]

The loading of molybdate species, which is controlled by the pH value of the impregnating solution, is an important factor for controlling the surface structure of molybdate. [64] The surface hydroxyl groups on the support are believed to play an important role in the adsorption of molybdate on the support. [53] The hydroxyl groups of the support either become deprotonated at high pH values or protonated at low pH values. The molybdate loading can be controlled by the pH values of the impregnating solution by charge compensation between the molybdate species and the surface hydroxyl groups. As shown in Table 1, the molybdate loading increases with decreasing the pH value. The PZC of MoO_3 is 1.5 while that of γ-Al_2O_3 is 8.0. The formation of the molybdate species on the support will decrease the "surface pH value ". With increasing Mo loading, the "surface pH value" decreases, and the octahedral molybdate species formed on the support. This can explain why more octahedral molybdate species are formed on the support with increasing the molybdenum loading.

During calcination the symmetric stretching mode of the Mo═O bond shifts to a higher frequency region (932 cm^{-1} in Figures 7 and 935 cm^{-1} in Figure 9) and the intensities of the asymmetric stretching modes of Mo−O−Mo bonds increase. (847 cm^{-1} in Figures 8 and 840 cm^{-1} in Figure 10) This demonstrates that some MoO_4^{2-} species polymerize into the octahedral species during the calcination. It has been suggested that a broadening and a red shift of the lowest energy transition absorption of molybdate are associated with the formation of larger size of the molybdate species. [55] The shifts of Mo−O−Mo transition absorption in Figures 2 and 3 also provide the evidence for the polymerization process during calcination.

The Mo═O stretching bands of all the samples in the calcined state are much broader as compared with that in the wet state. (see Figures 5, 7−10) For example, the Mo═O stretching band of the MoO_3/γ-Al_2O_3 (3) sample is between 900 and 1000 cm^{-1} after the calcination at 773 K, while it is a relatively narrow band for the wet sample. This is due to the interaction between the surface species or the surface species and the support after calcination. This is also because the final structure of the molybdate is a complex mixture comprising the tetrahedral and octahedral species in the wet sample.

It is suggested that the "surface pH value" decreases when the sample is calcined because the surface NH_4^+ decompose. [18] This is the case for the MoO_3/γ-Al_2O_3 prepared using the solution of $(NH_4)_6Mo_7O_{24}^{6-}$ (AHM). To avoid the change of the "surface pH value" during the calcination, the catalyst is prepared with the solution of Na_2MoO_4. As shown in Figure 11, the Raman spectra show the constant band position at 908 cm^{-1}, the characteristic mode of the tetrahedral molybdate species for the wet, dried, and calcined state. The fact that the band at 908 cm^{-1} does not shift during the calcination, indicating that the tetrahedral molybdate species are formed on the support in the wet state, do not aggregate into the octahedral species during the drying and the calcination. This suggests that the "surface pH value" is not changed because the surface Na^+, unlike NH_4^+, remains on the surface during the calcination. Therefore the "surface pH value" can be kept higher than 8.0. As a result, the tetrahedral species can be stabilized even after the calcination at 773 K. This leads us to the conclusion that the "surface pH value" is the important factor to govern the coordination structures of the surface species.

The assignments of the UV−vis diffuse reflectance bands of reference compounds, for example, sodium molybdate (Na_2MoO_4·2 H_2O), molybdenum trioxide (MoO_3), and ammonium heptamolybdate, are not always in agreeable in the literature.[43,50,51] Although the band between 230 and 260 nm is commonly assigned to the electronic transition absorption of the Mo═O bond of the tetrahedral species, it is also found in some spectra of octahedral species, such as MoO_3 or $Mo_7O_{24}^{6-}$. In this work, the absorption at 230−260 nm is detected in the UV−vis diffuse reflectance spectra of all samples. As shown in Figures 7 and 9, the Raman band at about 950 cm^{-1} is assigned to the octahedral molybdate. The double and triple frequency bands of 950 cm^{-1} are also detected owing to the resonance Raman effect. This implies that the band between 230 and 260 nm should be assigned to the Mo═O electronic transition absorption of tetrahedral as well as the octahedral molybdate. However, the intensity of the resonance Raman band attributed to the tetrahedral molybdate species is much stronger than that of the octahedral species. In other words, the laser line at 244 nm excites mainly the charge transfer of the tetrahedral molybdate, although the 244 nm line is also accessible to the electronic transition absorption of octahedral molybdate species. This is probably due to the nonradiation and fluorescence processes in the polymerized octahedral molybdate species.

Conclusions

1. UV resonance Raman spectroscopy is used to investigate the surface molybdate species formed during the preparation. To avoid the fluorescence interference and using the laser line with shorter wavelength, the sensitivity of the Raman spectroscopy is increased greatly. Furthermore, resonance Raman effect excited by the laser line at 244 and 325 nm not only increases the Raman sensitivity by several orders of magnitude, but also gives more information on the coordination structure of molybdate species.

2. UV resonance Raman spectra show that the species adsorbed on the support surface in the wet state are not always in agreement with that in the impregnating solution at different

pH values. At pH = 10.0, solely tetrahedral molybdate species are adsorbed on γ-alumina from the impregnating solution, while both tetrahedral and octahedral species are formed at pH = 6.0 in the wet state. The molybdate species in the solution and on γ-alumina in the wet state are identical at pH = 10.0 because the pH value of impregnating solution and the PZC (point zero charge) value of γ-alumina (8.0) are close. On the other hand, both the tetrahedral and octahedral molybdate species are derived on γ-alumina, although only the octahedral species is present in the impregnation solution at low pH value of 3.0. This is due to some surface basic OH groups on γ-alumina although the impregnating solution is acidic. We concluded that the structure of the surface molybdate species is controlled by the "surface pH value", which is a function of the pH value of the impregnating solution and the net pH value at PZC of the support.

3. During calcination some tetrahedral molybdate species aggregate into the octahedral species. The octahedral species is formed for MoO_3/γ-Al_2O_3 catalyst even with extremely low molybdate loadings, although all surface species is the tetrahedral form before the calcination. This is due to the decrease in the surface pH value when NH_3 comes off from the surface. The tetrahedral molybdate does not polymerize when the catalyst is prepared with the solution of Na_2MoO_4 because the surface pH value keeps almost constant. This further indicates that the "surface pH value" is a key factor for controlling the coordination structure of the surface molybdate species.

Acknowledgment. This work was supported by the National Natural Science Foundation of China (NSFC) for Distinguished Young Scholars (Grant 29625305).

References and Notes

(1) Thomas C. L. *Catalytic Processes and Proven Catalysts*; Academic Press: New York, 1970.
(2) Wachs, I. E. Segawa, K. *Characterization of Catalytic Materials*, Butterworth-Heinemann: Boston, 1992.
(3) Grange, P. *Catal. Rev.* **1980**, *21*, 135.
(4) Katzer, J. R.; Sivasubramanian, R. *Catal. Rev.* **1979**, *20*, 155.
(5) Shah, Y. T.; Cronauer, D. C. *Catal. Rev.* **1979**, *20*, 209.
(6) Giordano, N.; Meazzo, M.; Castellan, A.; Bart, J. C.; Ragaini, V. *J. Catal*. **1977**, *50*, 342.
(7) Louis, C.; Tatibou, J. M.; Che, M. *J. Catal*. **1988**, *109*, 354.
(8) de Boer, M.; Dillen, A. J.; Koningsberger, D. C.; Geus, J. W.; Vuurman, M. A.; Wachs, I. E. *Catal. Lett*. **1991**, *11*, 227.
(9) Smith, M. R.; Zhang, L.; Driscoll, S. A.; Ozkan, U. S. *Catal. Lett*. **1993**, *19*, 1.
(10) Spencer, N. D.; Pereira, C. J.; Grasselli, R. K. *J. Catal*. **1990**, *126*, 546.
(11) Banares, M. A.; Fierro, J. L. G.; Moffat, J. B. *J. Catal*. **1993**, *142*, 406.
(12) Ng, K. Y. S.; Gulari, E. *J. Catal*. **1985**, *92*, 340.
(13) Kakuta, N.; Tohji, K.; Udagawa, Y. *J. Phys. Chem*. **1988**, *92*, 2583.
(14) van Veen, J. A. R.; Hendriks, P. A. J. M.; Romers, E. J. G. M.; Andrea, R. R. *J. Phys. Chem*. **1990**, *94*, 5275.
(15) Luthra, N. P.; Cheng, W.-C. *J. Catal.* **1987**, *107*, 154.
(16) Edwards, J. C.; Ellis, P. D. *J. Am. Chem. Soc.* **1990**, *112*, 8349.
(17) Stencel J. M. *Raman Spectroscopy for Catalysis*; New York.
(18) Wachs, I. E. *Catal. Today* **1996**, *27*, 437.
(19) Gerhard, M.; Srinivasan T. K. K. *Catal. Rev.* **1998**, *40* (4), 451.
(20) Brown, F. R.; Makovsky, L. E.; Rhee, K. H. *J. Catal.* **1977**, *50*, 162.
(21) Brown, F. R..; Makovsky, L. E.; Rhee, K. H. *J. Catal*. **1977**, *50*, 385.
(22) Medema, J.; van Stam, C.; de Beer, V. H. J.; Konings, A. J. A.; Koningsberger, D. C. *J. Catal.* **1978**, *53*, 386.
(23) Knözinger, H.; Jeziorowski, H. *J. Phys. Chem*. **1978**, *82*, 2002.
(24) Jeziorowski, H.; Knözinger, H. *J. Phys. Chem*. **1979**, *83*, 1166.
(25) Zingg, D. S.; Makovsky, L. E.; Tischer, R. E.; Brown, F. R.; Hercules, D. M. *J. Phys. Chem.* **1980**, *84*, 2898.
(26) Wang, L.; Hall, W. K. *J. Catal*. **1980**, *66*, 251.
(27) Wang, L.; Hall, W. K. *J. Catal*. **1983**, *83*, 242.
(28) Stencel, J. M.; Makovsky, L. E., Sarkus, T. A., de Vries, J.; Thomas, R.; Moulun, J. A. *J. Catal*. **1984**, *90*, 314.
(29) Payen, E.; Kasztelan, S.; Grimblot, J.; Bonnelle, J. P. *J. Catal*. **1986**, *17*, 233.
(30) van Veen, J. A. R.; de Wit, H.; Emeis, C. A.; Hendriks, P. A. J. M. *J. Catal*. **1987**, *107*, 579.
(31) Hardcastle, F. D.; Wachs, I. E. *J. Raman Spectrosc*. **1990**, *21*, 683.
(32) Williams, C. C.; Ekerdt, J. G.; Jehng, Jih-Mirn; Hardcarstle, F. D.; Wachs, I. E. *J. Phys. Chem*. **1991**, *95*, 8791.
(33) Vuurman, M. A.; Wachs, I. E. *J. Phys. Chem*. **1992**, *96*, 5008.
(34) Kim, D. S.; Segawa, K.; Soeya, T.; Wachs, I. E. *J. Catal*. **1992**, *136*, 539.
(35) Li, C.; Stair, P. C. *Catal. Lett.* **1995**, *36*, 119.
(36) Li, C.; Stair, P. C. *Stud. Surf. Sci., Catal*. **1996**, *101*, 881.
(37) Li, C.; Stair, P. C. *Catal. Today* **1997**, *33*, 353.
(38) Li, C.; Stair, P. C. *Stud. Surf. Sci. Catal*. **1997**, *105*, 599.
(39) Jacoby, M. *Chem. Eng. News* **1997**, 44.
(40) Stair, P. C. and Li, C. *J. Vac. Sci. Technol.* **1997**, *A15*, 1679.
(41) Li, C.; Xiong, G.; Xin, Q.; Liu, J.; Ying, P.; Feng, Z.; Li, J.; Yang, W.; Wang, Y.; Wang, G.; Liu, X.; Lin, M.; Wang, X.; Min, E. *Angew. Chem. Int. Ed.* **1999**, *38*, 2220.
(42) Xiong, G.; Li, C.; Feng C.; Ying P.; Xin, Q.; Liu, J. *J. Catal.* **1999**, *186*, 234.
(43) Jeziorowski, H.; Knözinger, H. *Chem. Phys. Lett*. **1977**, *51*, 519.
(44) Ashley, J. H.; Mitchell, P. C. H. *J. Chem. Soc. A* **1968**, 2821.
(45) Ashley, J. H.; Mitchell, P. C. H. *J. Chem. Soc. A* **1969**, 2730.
(46) Mitchell, P. C. H.; Trifiro, F. *J. Chem. Soc. A* **1970**, 3183.
(47) Asmolov, G. N.; Krylov, O. V. *Kinet. Katal*. **1970**, *11*, 1028.
(48) Giordano, N.; Bart, J. C. J.; Vaghi, A.; Castellan, A.; Martinotti, G. *J. Catal*. **1975**, *36*, 81.
(49) Praliaud, H. J. *Less-Common Met.* **1977**, *54*, 387.
(50) Iwasawa, Y.; gasawara, S. *J. Chem. Soc., Faraday Trans*. **1979**, *75*, 1465.
(51) Gajardo, P.; Grange, P.; Delmon, B. *J. Phys. Chem*. **1979**, *83*, 1771.
(52) Gajardo, P.; Pirotte, D.; Grange, P.; Delmon, B. *J. Phys. Chem*. **1979**, *83*, 1780.
(53) Wang, L.; Hall, W. K. *J. Catal*. **1982**, *77*, 232.
(54) Iwasawa, Y.; Yamagishi, M. *J. Catal*. **1983**, *82*, 373.
(55) Fournier, M.; Louis, C.; Che, M.; Chaquin, P.; Masure, D. *J. Catal*. **1989**, *119*, 400.
(56) Williams, C. C.; Ekerdt, J. G.; Jehng, J. M.; Hardcastle, F. D.; Turek, A. M.; Wachs, I. E. *J. Phys. Chem*. **1991**, *95*, 8781.
(57) Parfitt, G. D. *Pure Appl. Chem.* **1976**, *48*, 415.
(58) Parks, G. A. *Chem. Rev.* **1965**, *65*, 177.
(59) van Veen, J, A. R.; Hendriks, P. A. J. M.; Romers, E. J. G. M.; Andrea, R. R. *J. Phys. Chem*. **1990**, *94*, 5275.
(60) Chiu, N.-S.; Bauer, S. H., Johnson, M. F. L. *J. Catal*. **1984**, *89*, 226.
(61) Clausen, B. S.; Lengeler, B.; Topso, H.; *Polyhedron*. **1986**, *5*, 199.
(62) Knözinger, H.; Ratnasamy, P. *Catal. Rev.-Sci. Eng.* **1978**, *17* (1), 31.
(63) Turek, A. M., Wachs, I. E., DeCanio, E. *J. Phys. Chem.* **1992**, *96*, 5000.
(64) Vuurman, M. A.; Wachs, I. E. *J. Phys. Chem.* **1992**, *96*, 5008.